Numerical prediction of cables fire behaviour using non-metallic components in cone calorimeter

Alain Alonso[a*], David Lázaro[a], Mariano Lázaro[a] and Daniel Alvear[b]

[a] *Universidad de Cantabria, Santander, Spain;* [b] *General Directorate of Industry, Energy and Mines, Government of Cantabria, Santander, Spain*

* Corresponding author: Alain Alonso. GIDAI Group, Universidad de Cantabria, Avda. Los Castros, s/n, 39005 Santander, Spain. alain.alonso@unican.es. https://orcid.org/0000-0002-0115-3039

David Lázaro. GIDAI Group, Universidad de Cantabria, Avda. Los Castros, s/n, 39005 Santander, Spain. david.lazaro@unican.es. https://orcid.org/0000-0002-8150-4838

Mariano Lázaro. GIDAI Group, Universidad de Cantabria, Avda. Los Castros, s/n, 39005 Santander, Spain. mariano.lazaro@unican.es. https://orcid.org/0000-0002-1008-694X

Daniel Alvear. General Directorate of Industry, Energy and Mines, Government of Cantabria, Santander, Spain. alvear_md@cantabria.es. https://orcid.org/0000-0002-7105-5282

Numerical prediction of cables fire behavior using non-metallic components in cone calorimeter

Electrical cables must fulfil the Construction Product Regulation (CPR) by testing them according to EN 50399. Nevertheless, an unfordable trial and error procedure could stem from the definition of new cables. To achieve a better understanding of fire behavior of cables, researchers have been using techniques such as bench and reduced scale tests and computational fire models result in a way to minimize trial and error process. The present work proposes the combination of bench scale tests, using cone calorimeters and fire simulation modelling. In a first step, the thermal characterization of the cable parts is carried out, and then, in a second step, use this data to model complete cable samples in cone calorimeter tests. The simulations are compared with experimental data of two already rated cables. This process is intended to discard erroneous configurations, which display in bench scale sings of misbehavior compared with rated cables. This would avoid the manufacture of the complete cable if the results do not fulfill the requirements, and eventually, proceed to its production and test in full-scale when they do. This work has been carried out with two multi-core cables and the materials they were made of, and the results showed: a) the inverse modelling process to characterize materials parts obtained a fairly accurate approach, with small inaccuracies in the peaks of the curves; b) two simulation models (simple and detailed) were able to reproduce in general terms the heat release rate curve, however they released more energy than experimental tests and some discrepancies in the peaks were observed. Despite its simplicity, simple model obtained results fairly close to the experimental curves and took less time to simulate.

Keywords: electrical cables; fire testing; cone calorimetric; inverse modelling; fire simulation; polymers

Introduction

Electrical cables must fulfil the Construction Product Regulation (CPR) enacted by the European Union 205/2011 since 2016. This regulation provides a framework in which the materials must satisfy a series of resistance limits and certain hazardous substances are avoided, i.e., all cables must be evaluated and classified under a single criterion. The standard UNE-EN 13501-6 (2015) establishes specifically the classification of electrical cables and how to obtain it through flame propagation test UNE-EN 50399 (2016). This regulation makes manufacturers to improve their cables, achieving a better performance. To do so, the improvement process could

involve a significant number of tests, in other words, it could become a lengthy and costly process such as trial-and-error process.

Therefore, it seems reasonable obtain some evidences of the fire behavior of the cable, in the early stages of the development of a new cable. Accordingly, the number of tests should decrease, shortening the trial-and-error process.

Nevertheless, the prediction of the combustion behavior of the cables is a complex issue due to the large number of phenomena involved. Firstly, the thermal decomposition of each of the components of the cables is highly dependent on the boundary conditions (Lázaro et al. 2019; Alonso et al. 2022), therefore, the layout of the cables and their geometry could also affect their fire behavior and the release of gases during the combustion their (Martinka et al. 2019).

There are several research techniques to study the combustion behavior of cables. For instance, bench scale tests analyzing small pieces of cables represent one of the most widely used tools for analyzing the fire behavior of materials. Thereby, tests can be carried out using single burning item-SBI (UNE-EN, 2021), Fire Propagation Apparatus-FPA (ASTM, 2013) or Cone Calorimeter (ISO, 2015).

The cone calorimeter tests are widely employed due to their versatility, i.e. the tests can be carried out under several radiance fluxes. Although tested samples are relatively small (100 × 100 mm^2 surface area), they are large enough to be considered them as a representative portion of the entire item. Among the literature, it can be highlighted (Meiner et al. 2018; Martinka et al. 2018; Magalie et al. 2018). The work of Meiner et al. analyzed the effects of the gaps between cables in the test holder and their influence on the energy released. The authors found that separating the cables, increased the time-to-ignition and the heat release rate (HRR). Furthermore, regardless of the heat flux, the cable sheath drives the first part of the HRR curves. However, the fire behavior of the cables is highly dependent on the heat flux. The study of Martinka et al. assessed influence of the space between the cables in the sample holder and the thermal conductivity of the material used as support for the unexposed surface of the sample. As a conclusion, the energy released increased when the gap between the cables grew and the thermal conductivity of the underlying material decreased. Magalie et al. studied the influence of several boundary test conditions such as heat flux level or number and spacing of cables and cable thermal properties. The authors found that the number of cables and their layout had influence on the HRR curve. If the number of cables increased, the first peak of heat release rate increased as well. However, the HRR curve was proportional to the number of tested cables. A larger distance between cables increases their exposed surface area accelerating the pyrolysis of their parts, i.e. the sheaths and the insulations. Other important conclusion was the great influence of the sheath thickness on the HRR curve.

These works highlight the wide variety of combustion behavior that can be assess by modifying the experimental tests conditions. For this reason, it is important to find a conservative method for obtaining the combustion behavior of the cables. To do so, several works have shown a precise approach considering various assumptions and simplifications for the execution of experimental tests, allowing define more test types and covering a wider variability of the boundary conditions.

In this sense, Gallo et al. developed a small-medium-scale test method replacing the cone heater by a cabin (400 × 400 × 630 mm) with a burner inside it (Gallo et al. 2017). They analyze the influence of the use of either the complete cable or its parts, measuring properties such as HRR peak, total heat released (THR) and fire growth rate (FIGRA), therefore, a useful prediction of

the behavior in full-scale was obtained. Girardin et al. modified the cone calorimeter apparatus swapping the cone heater by an enclosure for testing pieces of cable sheaths (size 500 × 23 × 1 mm)(Girardin et al. 2016). The study concluded that the outer sheathing had large influence, releasing more than 60% of the total heat released during the tests. Therefore, it was suggested to focus on this part for the development of new cables. Furthermore, authors obtained linear correlations between the developed bench-scale test and the large-scale EN 50399 considering pHRR, THR, and total damaged length.

Simulation models have proven useful for modelling and characterizing thermal decomposition processes. For instance, in Witkowski et al. the authors employed several simulation models such as Comsol Multiphysics and FDS to determine thermal and kinetic properties from thermogravimetric test and use them to elucidate the mass loss in mass loss calorimeter apparatus, both, thermogravimetric and mass loss calorimeter apparatus under an inert atmosphere (Witkowski et al. 2015). In Girardin et al. authors aimed to analyze and determine the thermal properties of materials in order to assess their influence on pyrolysis models. While thermal properties were acquired using thermogravimetric analysis and other techniques with similar scale, an inert atmosphere mass loss cone was used to analyze the mass loss rate of the sample. The numerical model well estimated the mass loss from gasification tests (Girardin et al. 2015). Nevertheless, these previous works only focused on representing the pyrolysis, not considering combustion reactions. Kempel et al. has also analyzed the capacity of prediction of two numerical tools (FDS and Thermakin) to model the mass loss rate of poly (butylene terephthalate) (PBT). To do so, authors validate simulation results with cone calorimeter tests, showing suitable approaches limited only by the formation of the residues (Kempel et al. 2012). These works studied only one material sheet, and did not deal either with more complex geometries or with the combination of different materials. More complex samples as cables have been also represented by computational models, as in Marti et al., where a particle finite element method (PFEM) was employed to represent fire behavior of cable in a tailor-made bench scale cabin obtaining that PFEM was able to closely predict the temperature (Marti et al. 2021). However, this work acquired the input parameters to define the cables from experimental tests and literature and did not propose a methodology to obtain them. The present work aims to represent cable fire behaviours using a slightly more complex geometry than a sheet of single material under oxidative atmosphere to consider material combustion reactions, proposing a methodology to achieve the input parameters that define the materials.

Having proved the effectiveness of computational models, next step would be to analyse the capability of these models calibrated using small-scale tests data so as to model tests in larger scale. In order to extrapolate the results to different conditions and to make a prediction of the combustion behaviour of the cables, computational models have shown a good ability to cope with them. In literature, several works can be found focusing on the thermal characterization of the materials and trying to replicate the experimental tests, either on bench scale or on larger scales. Matala et al., though computational simulations and inverse modelling, estimates the parameters for the pyrolysis modelling of two PVC cables from thermogravimetric analysis (TGA) and cone calorimeter tests (Matala et al. 2011). In this work, the effect of the reaction scheme on the mass loss simulated curves was compared with the experimental ones, obtaining large differences depending on which scheme is used in cone calorimeter tests. Hehnen et al. analyses the fire spread in horizontal cable trays and compares the results from simulations with

experimental tests (Hehnen et al. 2018). To characterize the non-metallic parts of cables, this works employed an inverse modelling approach basis on the results of experimental tests from micro scale calorimeter (MCC) and cone calorimeter, and the authors obtained a good correlation between heat release rate curves (HRR). These authors further developed the outcomes from their previous work and presented them in (Hehnen et al. 2020). As an interesting conclusion, the authors found that for the inverse modelling, the data from cone calorimeter tests with a heat flux of 50 kW/m^2 fits better than with a heat flux of 25 kW/m^2. The results obtained from cable tray simulations show that the fire extinguished earlier and the energy produced is higher than the cable tray experimental tests. Beji et al. (Beji et al. 2018) analysed the fire propagation in horizontal cable trays with PVC cables. The thermal properties and fire behaviour of PVC were estimated from cone calorimeter tests results. The authors conclude that the simulated fire pattern is similar to experimental tests, however, the cable tray simulations based on the information provided by cone calorimeter tests produced less energy and slower growth than experimental tests, i.e., less conservative results.

However, all these modelling works, with the exception of Girardin et al., were based on the experimental tests of the complete cables; accordingly, the design and construction of the complete cable is required. Therefore, the prediction of the fire response of the cables before their manufacture seems to be helpful so as to minimize the cost and time. Taking advantage of the possibilities of simulation tools, in the present work, the authors propose to characterize the cable materials separately (sheath and insulation), via inverse modelling. Then, based on this information, it is proposed to elaborate a virtual electrical cable and test it using two types of cone calorimeter simulation models. This work compares the results from both models and assess them with experimental cone calorimetric results of two multi-conductor cables. The simulation of cables and the comparison of their results with rated cables allows dismissing unsuitable cable configurations and materials that provide worse performance than rated cables. Since it is not necessary to manufacture discarded configurations, the method proposed in this paper reduces materials and time during the developing process of a new cable. Having said that, suitable configurations must be produced and tested to obtain their class.

Methodology and Materials

In order to meet the objective of this work, the authors carried out the following steps:

- 1st stage: cone calorimeter experimental tests for the cable parts (materials) were performed;
- 2nd stage: the inverse modelling process to obtain the thermal and kinetic properties of these parts (materials) were carried out;
- 3rd stage: involved the simulations of the cone calorimeter tests to cables (made with the above materials);
- 4th stage: cone calorimeter tests of cables were performed and the results were used to validate the cone calorimeter model.

Experimental tests

Experimental tests were carried out using a cone calorimeter apparatus (ISO, 2015). The cable parts, i.e. the sheath and the inner insulation, were tested using square samples with average thickness of 4,6 mm and 100 × 100 mm of area, as Figure 1a shows for the sheath. The unexposed face of the sample was insulated and over the exposed face, a sample retained grid was placed in order to prevent the swelling of the material. Every material was tested 3 times under 2 radiation flux levels: 50 and 75 kW/m^2 to ensure repeatability. The sheath is made of halogen-free thermoplastic polyolefin with flame retardant, with a density of 1570 kg/m^3, which makes that the average initial mass of the samples was approximately 72,8 g. The cable insulation is made of cross-linked polyethylene (XLPE), with density of 900 kg/m^3, therefore, the average initial mass of the samples was approximately 14 g.

Figure 1. Sheath sample tested in cone calorimeter: a) before, b) during and c) after.

Cone calorimeter tests to electrical cables were carried out following the procedure used in FIPEC project (Grayson et al. 2000),i.e.: a) the samples had a total length of 100 mm, b) the samples and were placed in the sample holder side by side, filling the total exposed surface of the sample holder; c) a sample retained grid was placed over these pieces; and d) the unexposed surface was insulated. Additionally, a high temperature resistant cement insulates the ends of the cables, preventing the inner heating due to contact of the cross section with the sample holder walls. Next Figure 2 shows the set-up for cone calorimeter tests of complete cables. Every cable was tested up to 3 times under radiant heat flux of 50 and 75 kW/m^2 to ensure repeatability.

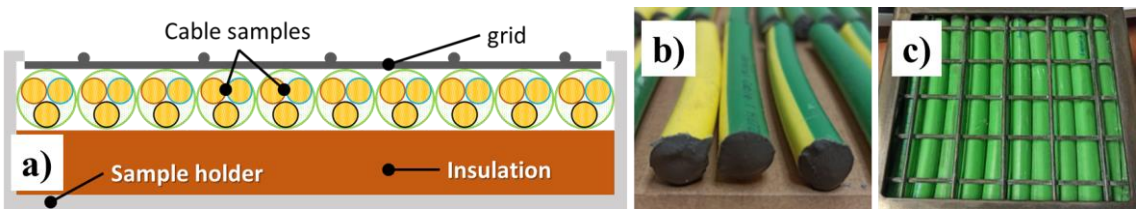

Figure 2. Complete cable samples in cone calorimeter test: a) drawing of layout, b) cable end insulation and c) cable samples placed in the sample holder before the test.

Two types of multi-conductor cables were tested, RZ1-K 3×1,5 mm^2 and RZ1-K 5× 1,5 mm^2 and their features are listed in Table 1.

Table 1. Features of tested samples.

Properties	RZ1-K 3 × 1,5 mm^2	RZ1-K 5 × 1,5 mm^2

Class	Cca-s1b,d1,a1	
Cable diameter (mm)	9,67	12,24
Sheath material	Halogen-free thermoplastic polyolefin	
Sheath thickness (mm)	1,72 ÷ 1,80	2,33 ÷ 2,39
Number of conductors / section (mm^2)	3 / 1,5 mm^2	5 / 1,5 mm^2
Conductor diameter (mm)	2,95	2,95
Insulation material	Cross-linked polyethylene XLPE	
Insulation thickness (mm)	0,82 ÷ 0,83	0,87 ÷ 0,93
Number of cable 100 mm pieces	10	8
Average initial sample mass (g)	135,9	179,5
Non-metallic mass (g)(%)	99,98 (73,57 %)	133,90 (74,6 %)
Mass sheath (g)(%)	83,86 (61,71 %)	105,72 (58,9 %)
Mass insulation (g)(%)	15,96 (11,75 %)	28,18 (15,7 %)
Metallic mass (conductors) (g)(%)	35,91 (26,43 %)	45,59 (25,4 %)

Inverse modelling process

To represent the thermal behaviour of any solid material using a computational model, it is necessary to introduce as input to the model, the values of the parameters that govern the thermal decomposition process, i.e., it is necessary to know or determine them previously. For this purpose, one of the most widely used methods is the inverse modelling process, allowing researchers to deduce the required parameters from experimental data (Lautenberger et al. 2011; Alonso et al. 2019, Hehnen et al. 2020). In the present work, the inverse modelling process was carried out combining: the shuffle complex evolution (from now on SCE) developed by the University of Arizona (Duan et al. 1993) as optimization algorithm and Fire Dynamics Simulator (FDS) developed by the National Institute of Standards (NIST) (McGrattan et al. 2022) as pyrolysis model. The process used MATLAB programing code (Matlab, 2018) for synchronize the SCE and FDS. The inverse modelling process is based on the work of (Alonso et al. 2019) , however, there were some differences. An inverse modelling process requires that the simulated cases achieve results with a certain degree of speed. Therefore, a very simple cone model was used consisting of: a solid representing the sample and a vent placed 25cm above the sample at the temperature that generated the desired level of radiation. Additionally, to enhance the computational speed, the gas phase of the model was deactivated, hence, the specific mass loss rate curve (sMLR) was measured. To obtain the heat release rate (HRR) curve the average value of the heat of combustion was used. Up to two heat fluxes were employed in order to include a wide thermal attack range. Every heat flux is evaluated according to next Eq. 1:

$$error_{HF} = \frac{\sqrt{\sum(x_{i\,exp} - x_{i\,sim})^2}}{\overline{x_{exp}}} \qquad (1)$$

where $x_{i\,exp}$ is the value of the specific mass loss rate curve at time i for the experimental test, $x_{i\,sim}$ is the same but for the simulated curve and $\overline{x_{exp}}$ is the average value of the specific mass loss rate experimental curve. The global evaluation function error for the three heat fluxes is as Eq. 2 shows:

$$global\ evaluation\ function\ error = \sqrt{(error_{HF50})^2 + (error_{HF75})^2} \qquad (2)$$

The process, displayed in Figure 4, can be briefly described as follows: 1) SCE chooses the values for the parameters of FDS input file; 2) the programming code generates the FDS input file and executed three simulations (same case but two different heat fluxes); 3) the global error is assessed based on Eq. 2; 4) if the stop criteria is not fulfilled the process resumes proposing a new set of values. The process is considered to be completed when either of these two criteria is fulfilled: 1) up to 20000 iterations as maximum or for five consecutive loops; 2) the value of Eq. 2 should no change more than 5 %.

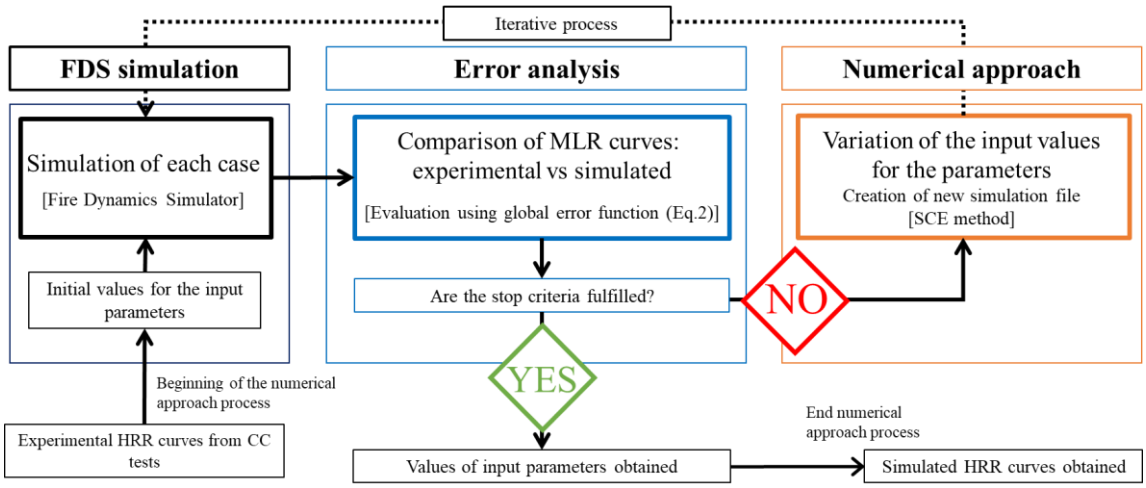

Figure 3. Scheme of numerical approach process.

The parameters included in the inverse modelling process were: emissivity (-), density (kg/m^3), conductivity (W/m·K), specific heat (kJ/kg·K), reaction order (-), Pre-exponential factor (1/s), activation energy (kJ/kmol), absorption coefficient (1/m), heat of reaction (k) (kJ/kg) and heat of combustion (kJ/kg). Basis on the results of Ghorbani et al. and Murer et al. (Ghorbani et al. 2013, Murer et al. 2018), a two consecutive reaction scheme was considered for the sheath which produced a considerable amount of char once the experimental test ends and one step reaction scheme for the insulation since the XLPE burned completely leaving any residue.

Computational modelling

Two models were built to simulate cone calorimetric tests (Figure 4): simple and detailed geometry model. Simple geometry model (for now on simple model) has two obstructions with a gap of 20 mm. The upper square obstruction is the heater and radiates the suitable level of heat flux towards the analyzed sample, represented by the lower obstruction. To radiate the required heat flux, the upper obstruction has a certain temperature, previously pre-calibrated following a process similar to the experimental one detailed in the standard (ISO, 2015). These temperatures were 743,5 ºC and 852,2 ºC, for 50 and 75 kW/m^2 heat flux levels respectively. To ensure a suitable balance between grid resolution and simulation time, the grid spacing considered was δ_x = 0,01 m.

The detailed geometry model (for now on detailed model) has a complex geometry and it reproduces with an accurate level the geometry of cone heater. Furthermore, the central hole allows the flame to develop and analyze the feedback of the flame. The gap between the heater and the tested sample (lower obstruction) is 25 mm, the same as cone calorimetric apparatus

indicated in standard ISO-5660-1 (ISO, 2015). As in the simple model, the temperatures of the upper obstruction were adjusted to measure in the center of the sample the intended heat flux, i.e., 802,7 ºC and 916, 4 ºC for 50 and 75 kW/m^2 respectively. This model had a cell size (δ_x) of 0,00625 m since the geometry required smaller cells than simple model.

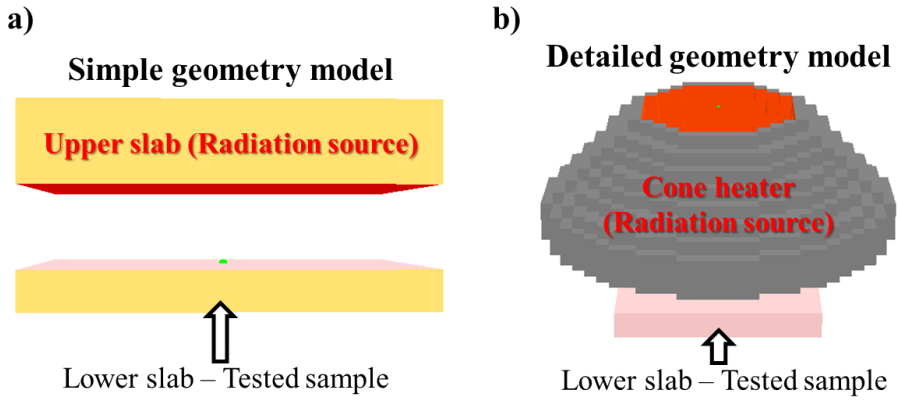

Figure 4. Computational models for cone calorimetric simulation: a) simple geometry, b) detailed geometry.

Between models, there was no difference in the lower slab to represent the cables. Cross sections of the cables were modeled as a continuous square solid made of different layers neglecting the metallic parts, i.e. the cupper conductors, as in (Matala et al., 2011). It had three layers: a) the upper one (exposed to radiation directly) stood for the sheath; b) the intermediate was a mixture of sheath and insulation and c) the bottom layer represented the lower sheath. This obstruction had the thermal and kinetic properties found via inverse modelling process (described in Table 4) and the emissivity was 0.9. Furthermore, the backside of the obstruction was insulated, i.e., no heat loss through this side was possible like in experimental tests. The criteria to determine the thickness of every layer of both cables was: a) layers corresponding to the sheath had the same thickness of the actual sheath; b) the intermediate layer had a thickness and proportion of materials in its mixture according to the actual amount and proportion of non-metallic materials. In summary, the initial amount of mass of each material was similar to that of the experimental tests. The features of the lower slab are summarized in next Table 2. In addition, the resolution of every cell passing through the slab was increased by dividing the thickness of each cell by 100.

Turbulence in both models was dealt with by LES (Large Eddy Simulation) mathematical model, using Deardorff Model (Deardoff coefficient = 0,1). The Near-Wall Turbulence Model was constant (Smagorinsky coefficient = 0,2) with Van Driest damping and Prandtl and Schmidt numbers were 0,5. Further details about how to set-up the model can be found in FDS user guide (McGrattan et al. 2022). The convective heat transfer was set to 10 W·m^2/K as is described in (Hopkins et al. 1996)(Rhodes et al. 1996).

Table 2. Properties of lower slab in cone calorimeter simulations

Properties / Cable	RZ1-K 3 × 1,5 mm^2	RZ1-K 5 × 1,5 mm^2
Upper layer thickness (mm)	1,75	2,30

Upper layer material	100 % sheath	100 % sheath
Intermediate layer thickness (mm)	3,20	5,00
Intermediate layer sheath proportion (%)	45,5	42,0
Intermediate layer insulation proportion (%)	54,5	58,0
Lower layer thickness (mm)	1,75	2,30
Lower layer material	100 % sheath	100 % sheath
Total non-metallic mass (g)	93,50	131,29
Sheath mass (g)	77,80	105,19
Insulation mass (g)	15,96	26,10

Results and discussion

This section gathers the results obtained for the experimental tests (cable parts and complete cables); inverse modeling process and cone calorimeters simulations. In order to display and compare them properly, they are grouped as follows: on the one hand, cone calorimeter experimental tests for cable parts and the inverse modelling results and on the other hand, cone calorimeter experimental tests for complete cables and their simulations.

Cone calorimeter tests for cable parts and inverse modelling

The sheath and the insulation were tested up to three times under flux levels of 50 and 75 kW/m^2. Next Figure 5 shows the heat release rate (HRR) curves for these tests.

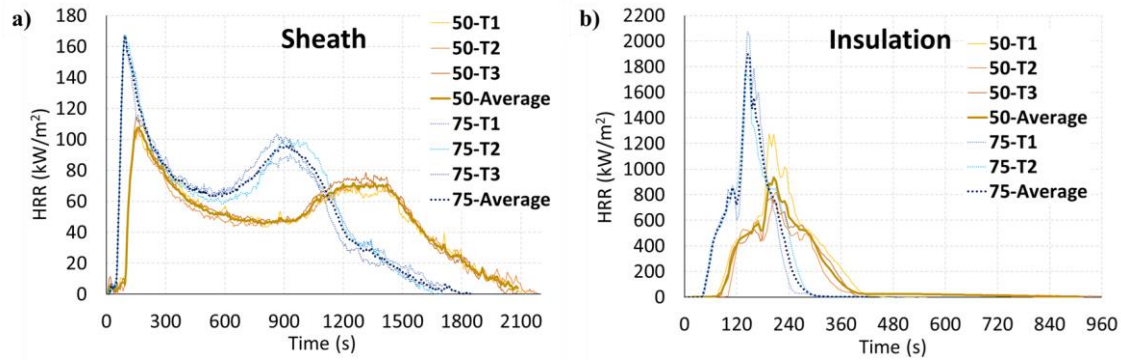

Figure 5. HRR curves of experimental tests for cable parts: a) sheath; b) insulation.

The sheath material HRR curves show two peaks: the first one was produced few seconds after the ignition, and the second one takes place prior to the flameout and before the descent period. Similar behaviour was observed between the two heat flux levels. The highest flux level causes the HRR curve to have higher values, but the tests took less time to finish. Increasing the heat flux level produced a larger amount of pyrolyzed gases released by the polymer decomposition. The opposite behaviour was observed when the samples are tested using the lowest flux level. Comparable amounts of energy are released in all six tests.

As far as the XLPE insulation is concern, a completely different behaviour was appreciated. Only one main HRR peak was produced for all tests. These peaks had the average values of 957,64 kW/m^2 for 50 kW/m^2 radiance level tests and 1916,35 kW/m^2 for higher heat flux level tests. As

the sheath tests, when the radiance level increased the HRR curve had higher values and the tests finished earlier. Regarding the total energy released, similar values were found between heat flux levels, although they were slightly larger when the heat flux level was 75 kW/m^2. The XLPE fluidized prior causing some of the sample to spill out of the sample holder.

The two average curves, for each material, were used for the inverse modelling process as target to adjust the simulated curves and determine the value of the set of parameters. Figure 6 and Table 3 show the results for the HRR simulated curves as results of the inverse modelling process compared with the experimental average curves. Finally, in Table 4 are listed the values of the parameters obtained by the inverse modelling process. Relative errors (%) made by the models are indicated in brackets.

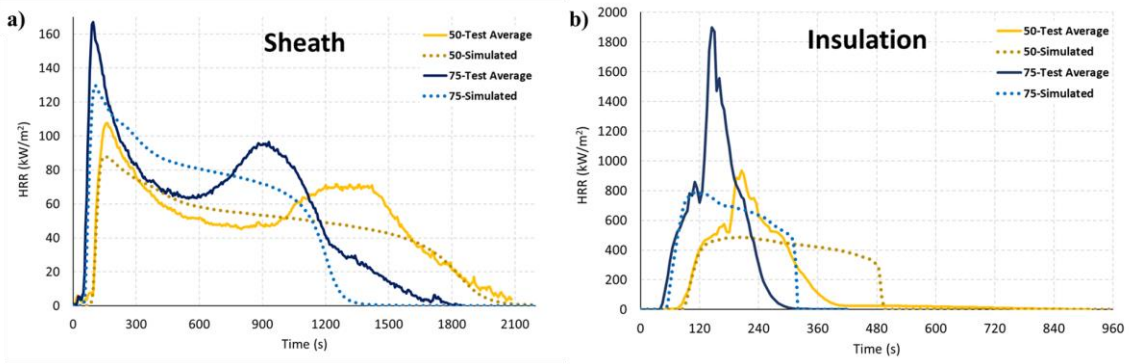

Figure 6. Obtained HRR curves for cable parts (experimental average and inverse modelling process): a) sheath, b) insulation.

As to the sheath, the HRR curves obtained by the inverse modelling were able to reproduce the instant ignition; but they had slightly smaller values for the first peak. On the other hand, the simulated curves did not achieve the same level of accuracy when the second HRR peak took place. The simulations released an amount of energy slightly higher than the experimental tests; therefore, the total mass loss was also higher than experimental tests. These differences between curves arise from the complex nature of the process as previously observed in (Hehnen et al. 2018),(Hehnen et al. 2020) and (Zhao et al. 2017). Despite these differences, the characterization obtained are valid to represent the global combustion process of the material and use it to represent the combustion process of the complete cable. The errors evaluated by Eq.1 for 50 kW/m^2 and 75 kW/m^2 were 5,60 and 7,14 respectively, hence, the global error (Eq. 2) was 9,8.

As far as the insulation is concern, simulated curves did not achieve the same level of accuracy as previous material. The simulated curves modeled correctly the ignition time and first instants of the upward HRR curve, up to the intermediate peak. At this point, there was a lack of sharpness in the reproduction of experimental HRR peak which led to increase the error, i.e., the experimental curves remained rising but not the simulated ones. This lack of accuracy in modelling of sharp peaks was previously appreciated in (Hehnen et al. 2018) and (Zhao et al. 2017) After the peak, it was also appreciated some differences. While the experimental curves had quasi-constant decrease rate, up to two rates were observed in simulated ones: slow and sudden decrease. These features these characteristics produced the next values for the errors (Eq. 1): 20,28 and 25,32 for 50 and 75 kW/m^2 respectively. The global error (Eq. 2) was 32,37.

Table 3. Values of tests for cable parts: experimental average (exp) and inverse modelling process (sim).

Properties	Sheath				Insulation			
	50 kW/m^2		75 kW/m^2		50 kW/m^2		75 kW/m^2	
	exp	sim	exp	sim	exp	sim	exp	sim
Time to ignition (s)	93	75 (19,3%)	48	45 (6,2%)	75	80 (6,67 %)	38	50 (31,6%)
1st HRR peak (kW/m^2)	108,8	87,9 (19,2%)	166,9	129,2 (22,2%)	957,6	484,9 (49,3 %)	1916,3	784,3 (59,1 %)
Time 1st HRR peak (s)	160	155 (3,3%)	95	155 (63,1%)	205	205 (0,0%)	145	120 (17,2 %)
Total Heat Released (THR)(kJ)	898,8	941,9 (4,8%)	885,80	943,8 (6,6%)	1241,9	1643,3 (30,3%)	1505,1	1643,5 (9,2 %)
Mass loss (%)	55,05	60,12 (9,2 %)	53,90	60,24 (11,7%)	79,98	99,24 (24,1%)	92,86	99,25 (6,5%)

Table 4. Thermal and kinetic properties obtained via inverse modelling process.

Parameters	Sheath			Insulation	
	Material 1	Submaterial 1	Residue	Material 1	Residue
Emisivity (-)	0,846	0,758	0,586	0,621	0,84862
Density (kg/m^3)	1570	960,4	622,67	900	6,9461
Conductivity (W/m·K)	2,205	3,112	1,945	1,098	0,54742
Specific heat (kJ/kg·K)	3,706	1,611	2,085	2,290	2,3633
Reaction order (-)	7,34	5,40	-	4,41	-
Pre-exponential factor (1/s)	4,8E+27	4,7E+27	-	7,7E+47	-
Activation energy (kJ/kmol)	264783	241915	-	543093	-
Absorption coeficient (1/m)	4,1E+09	3,8E+09	4,94E+09	6,9E+09	7,6E+09
Heat of reaction (kJ/kg)	3237	5015	-	2152	-
Heat of combustion (kJ/kg)	21231	21231	-	36075	-

All the values of Table 4 were used as input data for characterizing the materials of the cable in cone calorimeter simulations for complete cables described in next section.

Cone calorimeter tests for complete cables: experimental and simulations

Figure 7 displays the HRR curves of experimental tests of complete cable samples (and their average curves) for both heat fluxes.

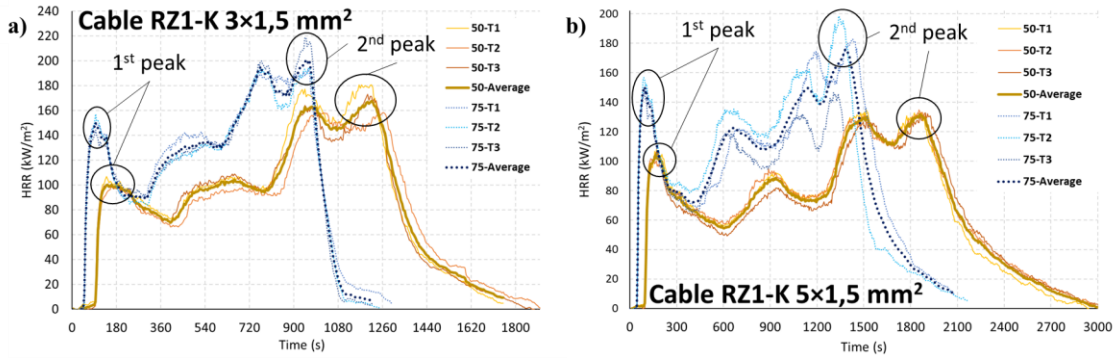

Figure 7. HRR experimental curves for complete cable samples: a) RZ1-K 3 × 1,5 mm^2, b) RZ1-K 5 × 1,5 mm^2.

As in cone calorimeter tests to cable parts, the higher heat flux level, the more HRR was produced. Overall, HRR curves for 50 kW/m^2 tests were similar to 75 kW/m^2 ones but rescaled, i.e. with smaller HRR values and delayed few seconds. Both cables had similar behavior: 1) a peak of HRR was produced few seconds after the ignition, and after it took place, the curve decreased up to a minimum; 2) the HRR values started to increase again up to reach the maximum value of the curve. In this part, the HRR curves had a "saw-tooth" profile with local maximums and minimums but showing an upward profile. Once the maximum value was reached, the curve decreased up to the flameout of the sample. Regarding the total energy released, for both cables and both heat fluxes, similar values were appreciated. However, for both cables, the heat flux determined how the energy was released. On the one hand, the lowest heat flux made the last longer producing smaller HRR values. On the other hand, the highest one generated more elevated HRR values but the tests were shorter.

The average HRR curves were employed for the comparison with the simulated curves obtained for the simple and detailed model. In Figure 8 and Table 5 are displayed the results for the cone calorimeter experimental tests and simulations to complete RZ1-K 3 × 1,5 mm^2 cable samples. Table 5 includes between brackets the relative errors (%) made by the models.

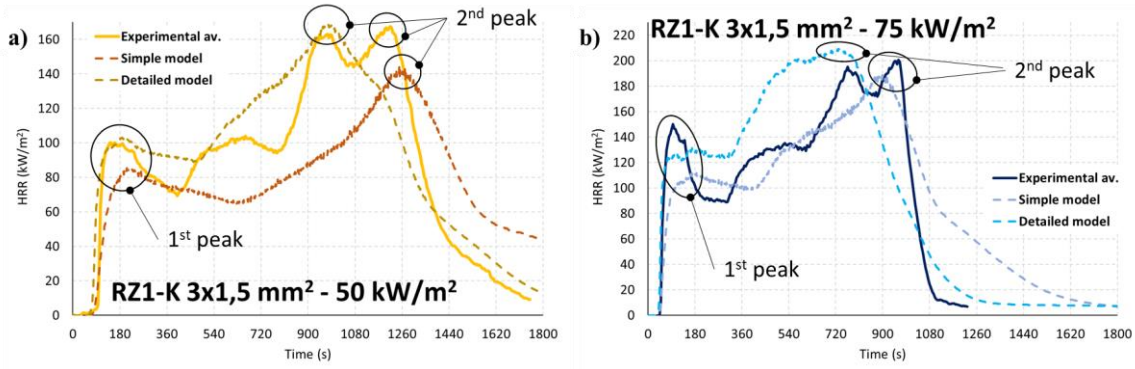

Figure 8. HRR curves of complete RZ1-K 3 × 1,5 mm^2 cable samples (experimental average and simulated): a) 50 kW/m^2, b) 75 kW/m^2.

Table 5. Values of tests for complete RZ1-K 3 × 1,5 mm^2 cable samples (experimental average and simulated).

Properties	50 kW/m^2			75 kW/m^2		
	exp	Simple model	Detailed model	exp	Simple model	Detailed model
Time to ignition (s)	88	61 (30,7%)	56 (36,4%)	44	36 (18,2%)	34 (22,7%)
1st HRR peak (kW/m^2)	102,6	84,5 (17,6%)	103,4 (0,8%)	145,9	110,6 (24,2%)	123,6 (15,3%)
2nd HRR peak (kW/m^2)	163,9	141,6 (13,6%)	168,5 (2,8%)	199,1	187,4 (5,9%)	207,0 (4,0%)
Time 1st HRR peak (s)	180	227 (26,1%)	202 (12,2%)	105	176 (67,6%)	86 (18,1%)
Time 2nd HRR peak (s)	1225	1258 (2,7%)	979 (20,1%)	965	902 (6,5%)	751 (22,2%)
Total Heat Released (THR)(kJ)	1355,2	1412,8 (4,3%)	1647,8 (21,6%)	1234,6	1597,7 (29,4%)	1649,8 (33,6%)
Mass loss (%)	39,29	57,86 (47,3%)	67,72 (72,4%)	40,20	64,6 (60,7%)	50,51 (25,6%)

As regards the 50 kW/m^2 heat flux, simulated curve obtained by the simple model reproduced the time ignition instant anticipating the instant 27 seconds, whereas the detailed one was 32 earlier. In general, simple model generated lower HRR values than experimental ones, with two peaks slightly delayed compared with the experimental results. On the contrary, the detailed model produced slightly higher HRR values than experimental test, which fitted better with the experimental curve than simple model. Accordingly, the detailed model produced less error (Eq .1) than simple one, i.e., 7,25 for simple model and 4,22 for detailed one. Overall, both models produced more total heat released and lost more mass than experimental tests, being the detailed model the one that releases more energy and loses more mass. As for 75 kW/m^2 heat flux, simulated curves had similar features than lowest heat flux. The errors (Eq. 1) with this flux were 4,43 and 5,68 for simple and detailed model respectively.

The detailed model fits better to experimental curves than simple in two stages of the simulation: a) up to the first peak was produced; b) after the last peak was produced, reproducing the descent of the HRR with similar rate and time. Furthermore, the detailed model produced peaks values more accurate than simple. Nonetheless, the simple model was more precise in describing the time to ignition and between first and last peak period. Even though HRR values produced by simple model were smaller than detailed model in this part of the test, the differences between experimental and simulated HRR curves were smaller for the simple model. Accordingly, the global error produced by both models and fluxes (Eq. 2) were 8,49 and 7,08 for simple and detailed model respectively.

The differences between the simulation results arose from the way in how the cone heater was modelled. In simple model, the gap between the heater and sample was 20 mm resulted in the flame was not be able to fully develop when it took place. As the radiation portion of the flame depends on its length, and therefore, the flame heat flux modifies the burning rate (Rhodes et al. 1996), the radiation from flame received by the sample was smaller. The detailed model did not have any obstacle right over the sample and the area of the heater was larger than the sample, accordingly, the feedback from flame radiation was higher than simply one.

Although the simple model produced smaller HRR values, the error produced (Eq. 1) was not as elevated as it could be expected due to the assumptions made. As the phase between the first and

the last peaks lasted approximately 60-70 % of the total testing time, the error accumulated by the simple model was similar to the detailed one.

total testing time, the error accumulated by the simple model was similar to the detailed one.

Next Figure 9 and Table 6 show the results obtained by the models for RZ1-K 5 × 1,5 mm^2 cable samples. In Table 6 are included the relative errors (%) made by the models.

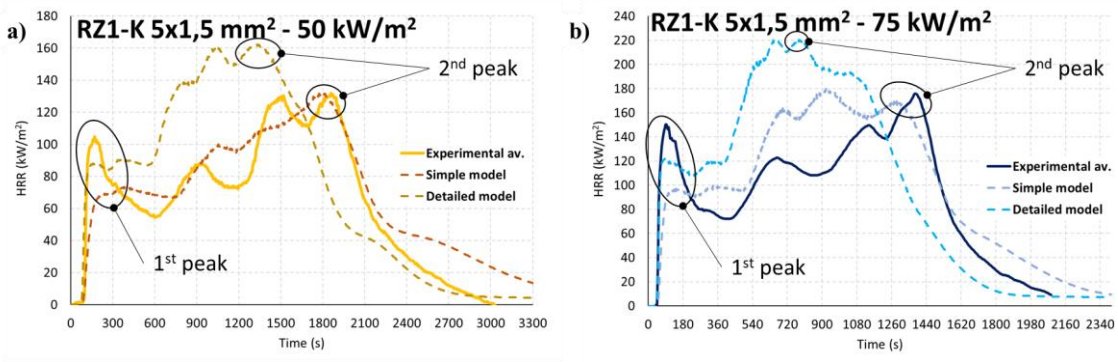

Figure 9. Comparison between HRR curves for cable RZ1-K 5 × 1,5 mm^2 cone calorimeter tests: a) 50 kW/m^2, b) 75 kW/m^2.

Table 6. Values of cone calorimeter tests for complete RZ1-K 5 × 1,5 mm^2 cable samples: average experimental and simulated.

Properties	50 kW/m^2			75 kW/m^2		
	exp	Simple model	Detailed model	exp	Simple model	Detailed model
Time to ignition (s)	93	72 (22,6%)	68 (26,9%)	42	40 (4,8%)	33 (21,4%)
1st HRR peak (kW/m^2)	106,3	68,2 (35,8%)	87,5 (17,7%)	148,2	95,1 (35,8%)	120,9 (18,4%)
2nd HRR peak (kW/m^2)	131,1	131,6 (0,4%)	162,1 (23,6%)	175,3	169,4 (3,4%)	219,6 (25,3%)
Time 1st HRR peak (s)	186	227 (22,0%)	166 (10,8%)	105	120 (14,3%)	98 (6,7%)
Time 2nd HRR peak (s)	1870	1800 (3,7%)	1346 (28,0%)	1390	1286 (7,5%)	748 (46,2%)
Total Heat Released (THR)(kJ)	1770,4	2301,1 (30,0%)	2449,1 (38,3%)	1718,1	2311,8 (34,6%)	2362,1 (37,5%)
Mass loss (%)	39,98	64,79 (62,1%)	70,66 (76,7%)	40,16	65,24 (62,5%)	71,41 (77,8%)

The results of both models and fluxes for RZ1-K 5 × 1,5 mm^2 cable had similarities with the previous one. For instance: 1) both models released more energy and lost more mass than experimental tests (the detailed one produced highest HRR values); 2) the ignition time of simulations was earlier than the experimental tests (the detailed model ignited faster than simple one). However, some differences were appreciated: 1) while the detailed model was more accurately fitted to the first HRR peak than simple model, the simple model better modeled the second peak; 2) after the second peak, the mass loss rate of the simple model was best suited to the experimental one. The global errors (Eq. 2) were 8,96 and 19,62 for simple and detailed model respectively.

As the other cable, the heater allowed the flame to extend its full length, as such; the heat received by the sample was higher than in the simple model. However, the heating process seemed to be excessively high for modelling the actual HRR curve.

Conclusions

The developing process of an electrical cable tends to involve several experimental tests that usually implies an effort in terms of materials, time and money. To reduce them, small-scale experimental tests and simulation tools are widely used. The present work proposes the use of the information provided by cone calorimeter tests to cable parts (individually), via inverse modelling process, and use it to build a virtual cable, test it and compare with cone calorimetric results to two actual cables. This procedure would represent an advantage during the developing process since, through a process of comparison with cone calorimeter test results of already manufactured (and classified) cables, not suitable configurations or materials could be discarded prior to build the new cable samples and test them in the cone calorimeter and full-scale (UNE-EN 50399). Afterwards, those configurations that obtained suitable results should be manufactured and tested in the calorimetric cone and eventually in full-scale.

In the light of the inverse modelling results, the combination of the SCE algorithm and FDS software (as pyrolysis model), allows obtaining the set of parameters that characterize the thermal decomposition process and combustion for sheath and insulation materials. These results were in line with previous works such as of Alonso et al. (2019) and Hehnen et al. (2020). However, it is worth pointing out that pyrolysis models have limitations predicting the thermal decomposition as is suggested in (Ghorbani et al. 2013) and (Bal et al. 2015). For instance, the remarkable HRR peak of insulation and the second one of the sheath were not quite as accurate as other parts in reproducing the experimental ones.

The simulation models elaborated were able to reproduce the experimental HRR curves from cone calorimeter tests using the samples of complete cable; however, they released a slightly higher amount of heat than experimental tests. In particular, each model has its pros and cons. A more realistic representation of the cone test, i.e. the detailed model, is bound to represent with more accurate level the first HRR peak (time and value) and produce higher HRR values than experimental tests. On the other hand, the simple model produced smallest HRR values than detailed model and experimental tests as well. Even though the simple model seemed to be too basic to represent the test, the value of the errors produced suggests that it use should not be dismissed. Actually, due to its short time to run the simulation, the employ of simple model the use seems to be a reasonable option to be considered before using the detailed one.

Having said that, the workflow exposed in this study should be tested with other cable configurations and materials. The results and conclusions that can be drawn from this work represent an interesting starting point for further analysis concerning the computational modelling of cables in cone calorimetric tests.

Acknowledgments

This publication is part of the R&D project RTC-2017-6066-8 funded by MCIN/ AEI/10.13039/501100011033/ and ERDF "Una manera de hacer Europa". The authors would like to thank to the Consejo de Seguridad Nuclear for the cooperation and co-financing the project "Metodologías avanzadas de análisis y simulación de escenarios de incendios en centrales nucleares". This work has been previously presented in 28th International Colloquium on the Dynamics of Explosions and Reactive Systems (ICDERS). The authors would like to be grateful to the organization for their collaboration.

References

Alonso, A., Lázaro, M., Lázaro, P., Lázaro, D., and Alvear, D. 2019. LLDPE kinetic properties estimation combining thermogravimetry and differential scanning calorimetry as optimization targets. *J Therm Anal Calorim* 138: 2703–2713. https://doi.org/10.1007/s10973 019-08199-4

Alonso, A., Lázaro, D., Lázaro, M., and Alvear, D. 2022. Self-heating evaluation on thermal analysis of polymethyl methacrylate (PMMA) and linear low-density polyethylene (LLDPE). *J Therm Anal Calorim*, https://doi.org/10.1007/s10973-022-11364-x

ASTM, E. 2013. 2058-13. Standard Test Methods for Measurement of Synthetic Polymer Material Flammability Using a Fire Propagation Apparatus (FPA). *Annu. Book Stand*. DOI: 10.1520/E2058-13

Bal, N, & Rein, G. 2015. On the effect of inverse modelling and compensation effects in computational pyrolysis for fire scenarios. *Fire Saf. J.*, 72; 68-76. https://doi.org/10.1016/j.firesaf.2015.02.012

Beji, T., & Merci, B. 2018. Numerical simulations of a full-scale cable tray fire using small-scale test data. *Fire Mater* 43(5): 486-496. https://doi.org/10.1002/fam.2687

Duan, Q. Y., Gupta, V. K., and Sorooshian, S. 1993. Shuffled complex evolution approach for effective and efficient global minimization. *J optimiz theory app* 76(3); 501-521. https://doi.org/10.1007/bf00939380

Grayson, S., Van Hees, P., Vercellotti, U., Breulet, H. and Green, A. 2000. Fire Performance of Electrical Cables – New Test Methods and Measurement Techniques. Final report of European Commission. SMT Programme Sponsored Research Project SMT4-CT96-2059. *Interscience Communications London*.

Gallo, E., Stöcklein, W., Klack, P. and Schartel, B. 2016. Assessing the reaction to fire of cables by a new bench-scale method. *Fire Mater* 41(6): 768-778. https://doi.org/10.1002/fam.2417

Ghorbani, Z., Webster, R., Lázaro, M. and Trouvé, A. 2013. Limitations in the predictive capability of pyrolysis models based on a calibrated semi-empirical approach. *Fire Saf. J.* 61, 274-288. https://doi.org/10.1016/j.firesaf.2013.09.007

Girardin, B., Fontaine, G., Duquesne, S., Försth, M., and Bourbigot, S. 2015. Characterization of thermo-physical properties of EVA/ATH: application to gasification experiments and pyrolysis modeling. *Materials*; 8(11), 7837-7863. https://doi.org/10.3390/ma8115428

Girardin, B., Fontaine, G., Duquesne, S. and Bourbigot, S. 2016. Fire tests at reduced scale as powerful tool to fasten the development of flame-retarded material: Application to cables. *J Fire Sci* 34(3): 240-264. https://doi.org/10.1177/0734904116642618

Hehnen, T., Arnold, L., Van Hees, P. and La Mendola, S. 2018. Simulation of Fire Propagation in Cable Tray Installations for Particle Accelerator Facility Tunnels. *Proc 8th International Symposium on Tunnel Safety and Security ISTSS*.

Hehnen, T., Arnold, L. and La Mendola, S. 2020. Numerical Fire Spread Simulation Based on Material Pyrolysis—An Application to the CHRISTIFIRE Phase 1 Horizontal Cable Tray Tests. *Fire* 3(3): 33. https://doi.org/10.3390/fire3030033

Hopkins, Jr D., and Quintiere, J.G. 1996. Material fire properties and predictions for thermoplastics. *Fire Saf. J.* 26(3), 241-268. https://doi.org/10.1016/S0379-7112(96)00033-1

ISO. 2015. 5660-1. Reaction-to-fire tests — Heat release, smoke production and mass loss rate — Part 1: Heat release rate (cone calorimeter method) and smoke production rate (dynamic measurement)

Kempel, F., Schartel, B., Linteris, G. T., Stoliarov, S. I., Lyon, R. E., Walters, R. N., and Hofmann, A. 2012. Prediction of the mass loss rate of polymer materials: Impact of residue formation. *Combust. Flame*; 159(9): 2974-2984. https://doi.org/10.1016/j.combustflame.2012.03.012

Lautenberger, C., and Fernandez-Pello, C. 2011. Optimization algorithms for material pyrolysis property estimation. *Fire Saf Sci* 10, 751-764.

Lázaro, D., Lázaro, M., Alonso, A., Lázaro, P. and Alvear, D. 2019. Influence of the STA boundary conditions on thermal decomposition of thermoplastic polymers. *J Therm Anal Calorim* 138: 2457–2468. https://doi.org/10.1007/s10973-019-08787-4

Magalie, C., Anne-Sophie, C., Rodolphe, S., Laurent, F., Emmanuelle, G. and Christian, L. 2018. Fire behaviour of electrical cables in cone calorimeter: Influence of cables structure and layout. *Fire Saf J*: 99: 12-21. https://doi.org/10.1016/j.firesaf.2018.05.001

Marti, J., Schartel, B., and Oñate, E. 2022 Simulation of the burning and dripping cables in fire using the particle finite element method. *J Fire Sci* 40(1): 3-25. https://doi.org/10.1177/07349041211039752

Martinka, J., Rantuch, P., Sulová, J. and Martinka, F. 2019. Assessing the fire risk of electrical cables using a cone calorimeter. *J Therm Anal Calorim* 135(6): 3069-3083. https://doi.org/10.1007/s10973-018-7556-5

Matala, A. and Hostikka, S. 2011. Pyrolysis modelling of PVC cable materials. *Fire Saf. Sci* 10: 917-930. http://dx.doi.org/10.3801/iafss.fss.10-917

Matlab. 2018. Version 9.4.0.813654 (R2018a). Natick, Massachusetts: The MathWorks Inc.

McGrattan, K., Hostikka, S., Floyd, J., McDermott, R., Weinschenk, C. and Vanella, M. 2022. Fire dynamics simulator technical reference guide volume 1: Mathematical model. *National*

Institute of Standards and Technology-NIST special publication 1018 (1). http://dx.doi.org/10.6028/NIST.SP.1018

McGrattan, K., Hostikka, S., Floyd, J., McDermott, R., Vanella, M. 2022. Fire Dynamics Simulator, Technical Reference Guide, Volume 3: Validation. *National Institute of Standards and Technology-NIST special publication* 1018 (3). http://dx.doi.org/10.6028/NIST.SP.1018

McGrattan, K., Hostikka, S., Floyd, J., McDermott, R., Vanella, M. 2022. Fire Dynamics Simulator, User's Guide. *National Institute of Standards and Technology-NIST special publication* 1019. http://dx.doi.org/10.6028/NIST.SP.1019

Meinier, R., Sonnier, R., Zavaleta, P., Suard, S., and Ferry, L. 2018. Fire behavior of halogen-free flame retardant electrical cables with the cone calorimeter. *J Hazard Mater* 342: 306-316. https://doi.org/10.1016/j.jhazmat.2017.08.027

Murer, L., Chatenet, S., Fontaine, G., Bourbigot, S. and Authier, O. 2018. Influence of model assumptions on charring polymer decomposition in the cone calorimeter. *J Fire Sci* 36(3): 181-201. https://doi.org/10.1177/0734904118761641

UNE. 2019. 13501-6. Fire classification of construction products and building elements - Part 6: Classification using data from reaction to fire tests on power, control and communication cables.

UNE. 2021. 13823. Reaction to fire tests for building products - Building products excluding floorings exposed to the thermal attack by a single burning item.

UNE. 2016. 50399. Common test methods for cables under fire conditions - Heat release and smoke production measurement on cables during flame spread test - Test apparatus, procedures, results.

Rhodes, BT, and Quintiere, JG. 1996. Burning rate and flame heat flux for PMMA in a cone calorimeter. *Fire Saf. J.* 26 (3), 221-240. https://doi.org/10.1016/S0379-7112(96)00025-2

Witkowski, A., Girardin, B., Försth, M., Hewitt, F., Fontaine, G., Duquesne, S., Bourbigot, S., and Hull, T. R. 2015. Development of an anaerobic pyrolysis model for fire retardant cable sheathing materials. *Polym. Degrad. Stab.*; 113, 208-217. https://doi.org/10.1016/j.polymdegradstab.2015.01.006

Zhao, G., Beji, T., Zeinali, D., and Merci, B. 2017. Numerical study on the influence of in-depth radiation in the pyrolysis of medium density fibreboard. In *15th International Conference Fire and Materials 2017*; 863-877.